Controlled structural damaging of multiwalled carbon nanotubes and graphene nanoplatelets by oxidation for stable nanofluids with enhanced thermal conductivity

Mauricio Pavía, Mélanie Emo, Patrice Estellé, Abdul Rahman Mohamed, Brigitte Vigolo

Controlled structural damaging of multiwalled carbon nanotubes and graphene nanoplatelets by oxidation for stable nanofluids with enhanced thermal conductivity

Mauricio Pavía[a], Mélanie Emo[a], Patrice Estellé[b], Abdul Rahman Mohamed[c], Brigitte Vigolo[a,*]

[a] Université de Lorraine, CNRS, IJL, F-54000 Nancy, France

[b] Univ. Rennes, LGCGM, F-35000 Rennes, France

[c] School of Chemical Engineering, Engineering Campus, Universiti Sains Malaysia, 14300 Nibong Tebal, Seberang Perai Selatan, P. Pinang, Malaysia

Corresponding author : Brigitte Vigolo ; Brigitte.Vigolo@univ-lorraine.fr

Keywords: multi walled carbon nanotubes; graphene nanoplatelets; covalent functionalization; stability; nanofluids; thermal conductivity

Abstract

Because thermal conductivity of carbon nanomaterials is inevitably lowered upon functionalization and functionalization is required to stabilize nanofluids, to meet the two criteria of thermal conductivity enhancement and homogeneous dispersion over time is still highly challenging for carbon nanomaterial based nanofluids. In this work, both multiwalled carbon nanotubes and graphene nanoplatelets have been covalently functionalized with different rates by refluxing in sulfuric acid/nitric acid of different concentrations (1, 3, 5 and 7 M). We show that a compromise can be found between thermal conductivity enhancement of carbon-based nanofluids (to maximize) and carbon structure damaging through functionalization (to minimize) while a stable dispersion is obtained. An in-depth

characterization by transmission electron microscopy, Raman spectroscopy, Fourier transformed Infra-red spectroscopy, thermogravimetry analysis and thermogravimetry analysis coupled to a mass spectrometer allow to evaluate both the applied functionalization efficiency and the structural damage undergone by each carbon nanomaterial. From the prepared nanofluids at 0.25 wt.% concentration, the best performance is achieved with MWCNT treated by an acid mixture of H_2SO_4/HNO_3 (1:1 volumetric proportion) at concentrations of 3 and 5 M where the thermal conductivity reaches an enhancement of 9.4 % at 20 °C and a dispersion stability over 5 weeks with no change in nanofluid absorbance. We have proved that the proposed approach allows to meet the two key criteria strongly desired for nanofluid design, leading to nanofluids with higher performances compared to other nanofluids prepared with carbon nanotubes treated with similar methods from the oxidized carbon nanotube family.

Abbreviations

DIW	Deionized water
EG	Ethylene glycol
TC	Thermal conductivity
CNTs	Carbon nanotubes
MWCNTs	Multiwalled carbon nanotubes
GNPs	Graphene nanoplatelets
TGA	Thermogravimetry analysis
MS	Mass spectrometer
FTIR	Fourier transformed infra-red spectroscopy
UV-Visible	Ultraviolet-visible
CCF	Carboxylated carbon fragments

1. Introduction

First reported in 1995, nanofluids were born from the mankind's need of having advance heat transfer fluids [1]. They are defined as conventional heat transfer fluids, generally deionized water (DIW), ethylene glycol (EG) or a mixture of both (the solvent used is named base fluid), containing nanoparticles or nanomaterials with one dimension lower than 100 nm [2].

Nowadays with the relentless increase of energy consumption, it is expected that nanofluids with superior heat transfer features are foreseen to be used in the near future mostly in industry engines [3] or renewable energy production systems like solar panels or electronic devices [4] requiring high thermal transfer ability or dissipation rates. The nanoparticles are dispersed in the base fluid with the aim of improving its overall properties, especially their thermal conductivity. Generally, the higher the intrinsic thermal conductivity (TC) or the specific heat capacity of the dispersed nanoparticles, the better the resulting thermal properties of the nanofluid.

One of the main objectives in nanofluid research field is to maximize the transfer of the intrinsic TC of the nanoparticles at the macroscopic scale of the nanofluid [5,6]. For this purpose, a compromise has to be reached since the designed nanofluids have to follow two conflicting requirements: to preserve the intrinsic thermal conductivity of the nanoparticles and to achieve their good dispersion and stability within the base fluid. Indeed, functionalization either covalent or non-covalent of the nanoparticles required to induce the nanomaterial dispersion is known to affect the thermal performances of the nanofluids [7–10]. Carbon nanomaterials are widely known to possess a combination of outstanding chemical and physical properties [11–14]. Besides, carbon nanotubes (CNTs) and graphene, which have a remarkable thermal conductivity and chemical stability, have been the subject of many studies [15–18]. By using carbon nanomaterials into nanofluids, their exceptional properties can be leveraged on a larger scale, resulting in great benefits in a macroscopic context.

Unfortunately, carbon nanomaterials are very hydrophobic and they present a high tendency to self-aggregate due to the existence of strong van der Waals forces which prevent their proper dispersion in most polar liquids. Therefore, to solve this issue, a chemical modification or functionalization of the carbon nanomaterial surface is compulsory. The non-covalent approach, consisting of using surfactants that adsorb onto the materials surface creating a

coating layer and promote its dispersibility, is a simple and a widely used way to disperse nanocarbons [19–21]. However, the surfactant can be an undesired contaminant as the coating layer hinders nanocarbon thermal transfer and at the same time, it increases the nanofluid viscosity [22,23]. Covalent functionalization helps to reduce the nanocarbon hydrophobicity by attaching functional groups on the material surface [24]. This modification, if it is weakly controlled, disrupts the nanoparticle structure which directly hinders its native properties, being the intrinsic thermal conductivity not an exception [25]. Different types of chemical treatment have yet been tested in the past for developing carbon-based nanofluids with a large varieties of base fluids[19,26,27].

Increasing the nanoparticle content in the nanofluid in order to compensate these negative effects would reflect higher TC, however it is counterproductive as the resulting viscous nanofluid would require a great pumping power to flow [22,28]. Whereas for the non-covalent method, reduction of the surfactant layer is prejudicial for the nanofluid stability as discussed above. In an applicative perspective of nanofluids, it is challenging to match the two expectations: good thermal properties and good dispersion stability. With the covalent approach, to find a compromise between the oxidative power and properties preservation appears as a smart strategy to follow. However, such study is delicate to deal with since carbon nanomaterial chemical reactivity depends on the kind and the characteristic of the employed nanocarbon and the strength of the functionalization treatment is not easy to evaluate [29,30]; a multi-technique characterization strategy is here essential.

Besides the TC enhancement, to obtain a high performance nanofluid, the nanomaterial proper dispersion and stability in the base fluid is mandatory, although this requirement is weakly boarded in literature [31,32]. Therefore, control and manage the functionalization degree is essential to design a material capable to fulfill the stability and TC requirements for nanofluids.

Here, we present how to obtain highly stable water-based nanofluids prepared with both oxidized CNTs and graphene and with good thermal conductivity. The behavior and the chemical reactivity of the modified CNTs and graphene are compared with regards to the resulting nanofluid thermal conductivity and stability over time. First, multiwalled CNTs (MWCNTs) and graphene nanoplatelets (GNPs) were functionalized following a widely reported functionalization treatment consisting of refluxing the MWCNT/GNP in a mixture of sulfuric and nitric acid [33–35]. In this work, different molar concentrations have been used so that the oxidative power could be tuned; such approach applied to the two different carbon nanomaterials is seldom reported in literature. The damaging degree of the treated samples was evaluated by transmission electronic microscopy (TEM) and Raman spectroscopy. In addition, Fourier transformed infra-red spectroscopy (FTIR), thermogravimetry analysis (TGA) and TGA coupled to a mass spectrometer (MS) served to determine the nature of the introduced chemical species on the nanomaterial. Later, the functionalized nanoparticles (0.25 wt.%) were used to prepared nanofluids by the two-step method using DIW as base fluid. The quality of the dispersion was evaluated by ultraviolet-visible (UV-Visible) spectroscopy. An optimized functionalization rate of MWCNTs is found, allowing both limitation in the CNT structural damage, and promoting at the same time their dispersibility and stability in the base fluid, and the thermal conductivity (at 20 °C) of the nanofluids. This compromise cannot be not obtained with GNP. It appears though, that for the applied oxidative method, it cannot be reached here under the used range of chemical reaction strengths.

2. Materials and methods

2.1 Materials

The employed starting MWCNTs were synthesized by a CCVD process which took place at the Universiti Sains Malaysia facilities. As catalyst, Co-Mo and MgO were used. As

purification treatment, the produced tubes were stirred in nitric acid at 60 °C for 30 min to remove the remaining catalyst components without introducing functional groups. The resulting nanotubes possess 12 to 16 walls with an average diameter of 7 nm [36] and have a length not higher than 10 μm, estimated from TEM observations.

In the case of graphene, pristine GNP was furnished by Sigma Aldrich France. According to the manufacturer, GNPs possess an average length of 5 μm and a surface area between 120-150 m^2g^{-1} and 15 to 20 layers.

For the oxidative treatments, sulfuric acid (H_2SO_4), nitric acid (HNO_3), hydrochloric acid (HCl) and sodium hydroxide (NaOH) were purchased from Sigma Aldrich and used as received.

2.2 Oxidative treatments

The oxidative treatment involved the two samples to be submitted into reflux with an acid mixture of H_2SO_4/HNO_3, at concentrations of 1, 3, 5 and 7 M in a 1:1 volumetric proportion. Initially, 300 mL of the acid mixture were poured in a 500 mL round flask. Then, 300 mg of the departing sample were added. The flask was let to heat up at 110 °C in an oil bath and once the reflux started, it was let for 24 h. After, the flask was retired from the oil bath and set to cool down. Once room temperature was reached (RT), the product was filtered and rinsed with DIW, then it was sonicated during 30 min in 150 mL of a NaOH solution at 4 M to eliminate potential carboxylated carbon fragments (CCF) [37]. Then, the product was filtered and 250 mL of diluted HCl were added. Finally, sample was rinsed with DIW until neutral pH was reached and set to dry with the help of a freeze drier during 4 days. Each functionalization treatment was replicated at least 3 times for both starting samples.

Nanofluids were prepared with a representative 0.25 wt.% concentration of the treated MWCNT or GNP. Each sample was prepared at least twice. For all cases, DIW, without any additive or surfactant, was used as base fluid. The nanoparticles were dispersed in the base

fluid with the help of a sonication probe (Sonics Vibra-Cell VCX750 equipped with a CV334 probe) during 30 min at 20 °C in a cyclic mode (2 sec on, 1 sec off) at 300 W . To avoid heating and evaporation, the nanofluid container was put in ice bath during the sonication. Sample nomenclature is displayed in Table 1 to differentiate the type of carbon nanostructures and the oxidative treatment strength.

Sample nature	**Sample name**	**H_2SO_4/HNO_3 (1 M)**	**H_2SO_4/HNO_3 (3 M)**	**H_2SO_4/HNO_3 (5 M)**	**H_2SO_4/HNO_3 (7 M)**
MWCNT	SNT	NT-1M	NT-3M	NT-5M	NT-7M
GNP	SG	G-1M	G-3M	G-5M	G-7M

Table 1 Sample nomenclature.

2.3 Nanomaterial characterizations

For the TEM observations, the starting and oxidized nanotubes and graphene powder were dispersed in ethanol and gently sonicated in a sonication bath (Fisherbrand, Elmasonic S, 95 W, 37 kHz) during 5 min. A droplet of the prepared dispersion was placed on a copper grid covered with a holey amorphous carbon film (200 mesh size). The TEM micrographs were obtained using a JEOL JEM-ARM 200F Cold FEG apparatus equipped with a spherical aberration (Cs) probe corrector working at an accelerating voltage of 80 and 200 kV for the MWCNT and GNP observations, respectively. In this work, the TEM figures were prepared with selected MWCNT and GNP images representative of each sample from a batch of ca. 40 images obtained at different places randomly selected on the TEM grid for the same sample.

The TGA analysis was performed with the help of a Setaram Setsys evolution 1750. The analysis was made by increasing temperature from 20°C to 900°C (5 °C/min) under

166 controlled air flow (20 mL/min). In the context MS analysis, the TGA apparatus was linked
167 with a Pfeiffer GSD 301C Vacuum PrismaStar mass spectrometer. As before, the temperature
168 was raised from 20°C to 900 °C (5 °C min^{-1}). However, in this case the analysis was
169 conducted under a helium flow (20 mL min^{-1}).
170 Micro-Raman spectroscopy was carried out with a Jobin Yvon LabRAM HR800 equipped
171 with a CCD detector cooled to -70 °C. A 633 nm laser wavelength was used as the incident
172 beam focused on the sample with a microscope through a wide length x100 objective and a
173 numerical aperture of 0.50. For each sample, at least 8 spectra were recorded from different
174 spots. For each spectrum, the background was subtracted and the maximum intensity of the D
175 and the G bands were used to calculate the D intensity over the G intensity ratio, I_D/I_G. The
176 spectra with the closest values of the average I_D/I_G was chosen to be displayed.
177 A Nicolet 6700 FT-IR (Thermo Scientific) spectrometer was used for FTIR spectrometry
178 investigations. At least 5 spectra of each sample were recorded in ATR mode (diamond
179 crystal) using 100 scans and a resolution of 2 cm^{-1}.
180 **2.4 Thermal conductivity measurements**
181 The thermal conductivity measurements of the prepared nanofluids were carried out in several
182 replicates at 293.15 K (20 °C) with a THW-L2 device (Thermtest Inc., Richibucto Road, NB,
183 Canada) using the transient short hot-wire method according to the ASTM D7896 standard,
184 similarly to the procedure developed in [38]. In the temperature range 283.15 to 313.15 K, the
185 experimental uncertainty of the device has been evaluated from DIW water measurement after
186 probe calibration. These data have been compared to reference values for DIW. As an
187 experimental uncertainty evidence, an average absolute deviation (AAD) around 1 % in the
188 temperature range of 283.15 to 313.15 K has been obtained. This result is similar the AAD of
189 1.1 % reported by Prado *et al.* [39] with the same device, fluid and temperature range. Each
190 thermal conductivity value reported later is an average of at least 10 measures.

2.5 Nanofluid stability investigation

The UV–visible spectrophotometry of the nanofluids has been carried out with a Varian Cary7000 spectrophotometer in the 200–700 nm range using quartz cuvettes (28-F/Q/10) with an optical path of 2 mm furnished by Jasco France. As commonly found for such absorptive materials [40–42] , the nanofluids were first diluted 1:10 and the absorbance of the dispersion was measured by using a double beam mode and deducting the absorbance of the base fluid served as reference. Sample relative absorbance was compared at 500 nm [43,44] and followed during 35 days.

To sum up, the principle of nanomaterials and nanofluids preparations and characterizations methods are gathered in Fig. 1.

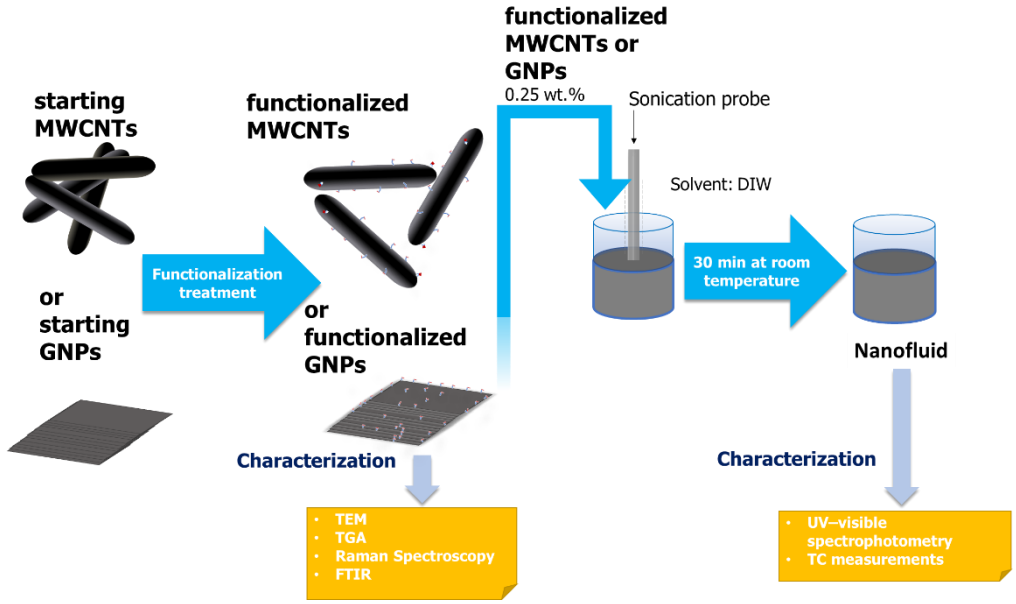

Figure 1. Schematic representation of the method to prepare nanofluids with oxidized MWCNT and GNP. Starting samples were first functionalized and then dispersed in the base fluid for the nanofluid preparation.

3. Results and Discussion

3.1 Morphological, structural and chemical study of the oxidized MWCNTs and GNPs

The TEM observations of starting MWCNTs and GNPs as well as their oxidized counterpart are shown in Figure 2.

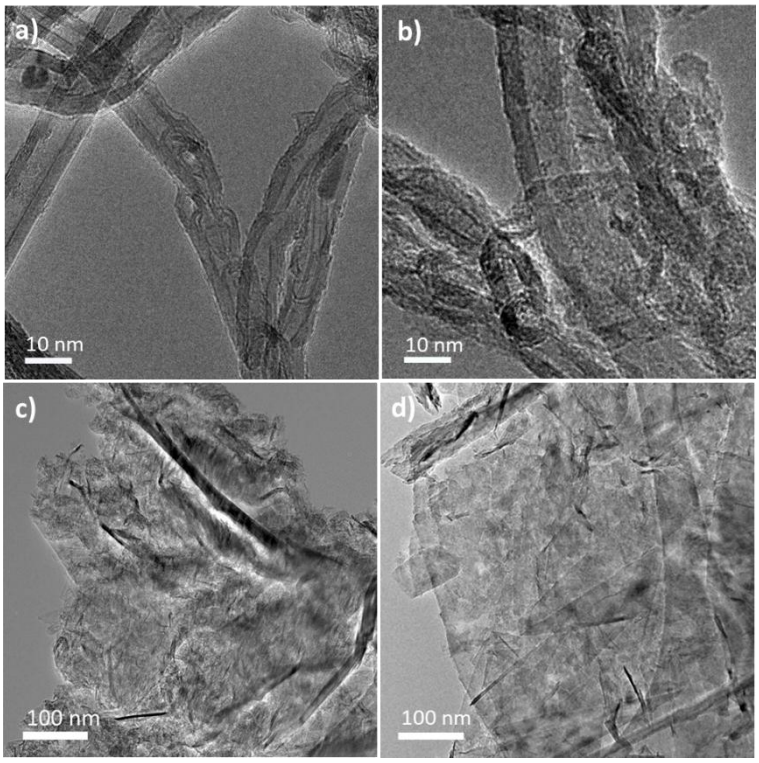

Figure 2 Typical TEM micrographs of a) starting MWCNTs (SNT), b) functionalized MWCNTs by H_2SO_4/HNO_3 at 7 M (NT-7M), c) pristine GNPs (G) and d) functionalized GNPs by H_2SO_4/HNO_3 at 7 M (G-7M).

Some embedded tubes are noticeable in the starting MWCNTs (SNT) and functionalized MWCNTs by H_2SO_4/HNO_3 with 7 M concentration (NT-7M) in Figs. 2a and 2b. From Figs. 2c and 2d, some wrinkles are typically detectable on the pristine GNPs (SG) and GNPs

functionalized with H_2SO_4/HNO_3 at 7 M (G-7M). For both GNP and MWCNT samples, the carbon structure seems of good quality without visible damaging which is certainly the sign that the applied treatment with H_2SO_4/HNO_3 at 7 M, even at high concentration, does not strongly attack the carbon network and avoids formation of breaks or holes in MWCNT walls and GNP layers. Both used carbon nanomaterials, MWCNT and GNP, possess a relatively high number of graphene sheets in their structure, around 15 for the first and 15 to 20 for the GNP (in agreement with the respective suppliers) which stabilizes them towards the applied chemical attack.

TGA is considered as an important technique for the nanocarbon study; the combustion temperature is sensitive to their structural properties in the sense that if their structure is damaged, for a similar content of inorganic impurities, the combustion temperature is downshifted to lower values. Fig. 3 shows the thermograms of the starting and oxidized MWCNTs and GNPs.

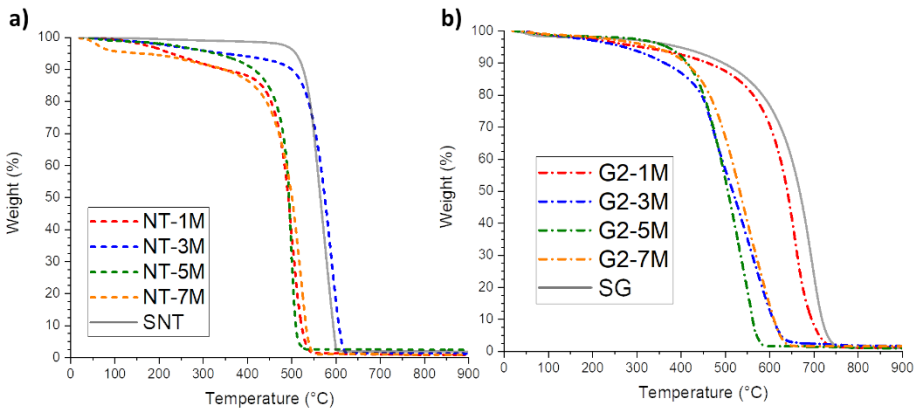

Figure 3 Thermograms under dry air of a) the starting and treated MWCNTs by H_2SO_4/HNO_3 at 1, 3, 5 and 7 M (SNT, NT-1M, NT-3M, NT-5M and NT-7M) and b) the starting and treated GNPs by H_2SO_4/HNO_3 at 1, 3, 5 and 7 M (SG, G-1M, G-3M, G-5M and G-7M).

A weak weight loss visible at around 100 °C for NT-7M is related to the moisture release by the nanocarbons. For the oxidized MWCNTs, another small weight loss is detected at around

250 °C, it corresponds to the removal of the oxygen-containing groups [45]. For all the samples, the main weigh loss due to the carbon specie combustion is located in the 450-750 °C range. From a general observation, the burn off temperature of both the oxidized MWCNTs and GNPs is downshifted compared to that of the respective starting unoxidized carbon nanomaterial. Such behavior is commonly detected in oxidized nanocarbons and it is strongly related to their structural quality since introduction of functional groups increases *de facto* their structural defects [34]. After combustion, the remaining weight in starting and treated MWCNTs and GNPs is in the 1-2 wt.% range which shows the good purity of both carbon nanomaterials (Figs. 3a and 3b). The starting MWCNTs (SNT) burn at around 600 °C (Fig. 3a). A shift towards lower combustion temperatures becomes evident as sample gets oxidized at 1 M, 5 M and 7 M. Apparently, without any explanation yet, this tendency is not followed by the MWCNTs functionalized with H_2SO_4/HNO_3 at 3 M (NT-3M) which

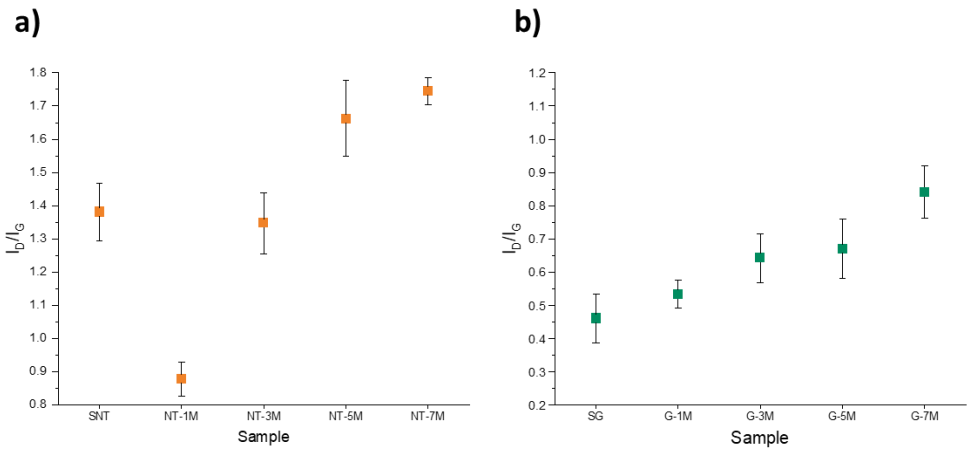

decomposes in a similar temperature range than that observed for the starting MWCNTs. The combustion of the starting GNP (SG) occurs around 700°C (Fig. 3b). Nonetheless, as the GNP sample gets functionalized there is a shift of more than 100°C towards lower combustion temperature for the samples treated with the acid mixture concentration at 3, 5 and 7 M (G-3M, G-5M and G-7M, respectively). This downshift is significantly smaller for the GNPs treated with the acid mixture solution at the lowest concentration (G-1M).

Figure 4 Raman spectroscopy I_D/I_G values of a) starting and treated MWCNT samples by H_2SO_4/HNO_3 at 1, 3, 5 and 7 M (SNT, NT-1M, NT-3M, NT-5M and NT-7M) and b) starting and treated GNPs samples by H_2SO_4/HNO_3 at 1, 3, 5 and 7 M (SG, G-1M, G-3M, G-5M and G-7M).

Raman spectroscopy is a mandatory characterization technique for carbon nanomaterials since it provides information about their integrity and it can serve to probe any structural modification introduced into the MWCNTs and GNPs. Typically the so called "G band" (around 1590 cm^{-1}) comes from the stretching of the C-C bonds of the sp^2 network. Moreover, the presence of disorder or defects in the sp^2-hybridized carbons is shown in the so called "D band" (around 1330 cm^{-1}) intensity. To have a more accurate idea of the "defects" introduced in the carbon nanomaterial framework, it is often suggested to divide both bands intensity in order to obtain the parameter I_D/I_G and compare it before and after oxidation. Besides, as the functionalization treatment modifies the carbon atom hybridization from sp^2 to sp^3 (defect) by introduction of chemical groups in the carbon network, I_D/I_G is affected. Representative Raman spectra of each sample are given in Fig. S1 (Supporting Information) and their corresponding I_D/I_G is displayed in Figs. 4a and 4b for the MWCNTs and GNPs, respectively. As expected for both cases, an increase in acid concentration during the oxidation treatment leads to a corresponding increase in the I_D/I_G [29], being the highest for the samples treated with the acid mixture at 7 M, *i.e.* 1.75 (± 0.04) for MWCNT (NT-7M) and similarly for GNP treated with the acid mixture at 7 M (G-7M), as an I_D/I_G of 0.84 ± 0.08 is obtained. For the MWCNTs treated with the acid mixture at 5 M and 3 M I_D/I_G values of 1.66 ± 0.11 and 1.35 ± 0.09 were found (Fig. 4a). The MWCNTs treated with H_2SO_4/HNO_3 with 1 M (NT-1M) displays a particular behavior since its I_D/I_G is lower than that of the starting MWCNTs. It has

been reported that this behavior is due to some kind of "cleaning effect" attributed to the removal of a thin disordered carbon layer at the MWCNT surface [46]; this effect is probably overcompensate by the introduction of defects due to functionalization when the acid treatment is strengthened. It should be noted that such effect is far less pronounced for graphene since this latter leads to a less pronounced resonant effect in Raman spectroscopy than CNTs [47]. In the case of the graphene samples, by lowering the oxidation strength, lower I_D/I_G values of 0.67 ± 0.09, 0.64 ± 0.07 and 0.53 ± 0.04 corresponding to samples treated by the H_2SO_4/HNO_3 mixture at 5 M (G-5M), 3 M (G-3M) and 1 M (G-1M) were found.

TGA-MS under inert atmosphere (helium) was also performed over the starting and oxidized MWCNTs and GNPs. If successful, the H_2SO_4/HNO_3 treatment will anchor oxygen-containing functional groups which will decompose and produce CO (m/z 28) and CO_2 (m/z 44) detected by the MS as temperature rises. The recorded weight loss and the corresponding MS signal for each oxidized MWCNTs and GNPs are given in Figs. S2 and S3 (Supporting Information), respectively. The temperature at which these CO/CO_2 species are detected can be assigned to specific functional groups as gathered in Table 2 [48].

Table 2 Assignment and quantification in wt.% of the oxygen containing functional groups detected at the MWCNT and GNP surface after oxidation by the acid mixture H_2SO_4/HNO_3 at 1, 3, 5 and 7 M concentration from TGA coupled with MS.

Sample	**Detected m/z**	**Functional group identified**	**Weight loss temperature (°C)**	**Weight loss (%)**
NT-1M	28	ether	750	0.38
NT-3M	44, 28	carboxylic	200-300	1.29

	44, 28	anhydride	600-700	0.86
NT-5M	44, 28	carboxylic	200-300	1.62
	44, 28	anhydride	600-700	1.51
	28	ether	720	0.62
	28	quinone	850	0.65
NT-7M	44, 28	carboxylic	200-300	1.84
	44, 28	anhydride	600-700	2.04
	28	ether	720	0.97
	28	quinone	850	0.48
G-1M	44,28	lactone	450	0.94
G-3M	44, 28	lactone	450	1.36
G-5M	44, 28	carboxylic	200-300	1.01
	28	quinone	700-850	2.59
G-7M	28	quinone	850	2.08

For the treated MWCNTs with the acid mixture at 3, 5 and 7 M (NT-3M, NT-5M and NT-7M respectively) and GNPs treated with 5 M of the acid mixture (G-5M), CO_2 (as the parent specie with CO as fragment) detected in the low temperature range; *i.e.* 200-300 °C, are assigned to carboxylic group species at around 1-2 % for the above samples. The GNPs oxidized with low strength (G-1M and G-3M) exhibit the presence of lactone (~450 °C) whose content increases with acid concentration (0.94 and 1.36 wt.% for G-1M and G-3M, respectively). At higher temperature, in the 600-700 °C domain, anhydride is evidenced from the observed CO_2/CO signal for the MWCNTs treated with 3, 5, 7 M of H_2SO_4/HNO_3; their content increases gradually as the treatement is strenghten (0.86, 1.51, 2.04 wt.% for 3, 5, 7 M,

315 respectively). From the detection of CO at 700 °C, a small amount of ether (less than 1 wt.%)
316 can be identified on most of the oxidized MWCNTs. For the highest used concentrations (5
317 and 7 M), quinone is detected (~850 °C) for NT-5M, NT-7M, G-5M and G-7M at a higher
318 amount for GNPs (more than 2 wt.%) than MWCNTs (around 0.5 wt.%).
319 FTIR was performed over the starting and oxidized samples to identify the nature of the
320 functional groups present at the material surface. The presence of oxygen-containing groups
321 that will promote the MWCNTs and GNPs hydrophilic character is expected [33]. From the
322 employed functionalization method, these groups contain mainly C-O, COOH and C=O
323 bonds [34]. Fig. 5 shows FTIR spectra of the raw and oxidized MWCNTs and GNPs. As
324 expected, the characteristic black bone (C=C) stretching vibration of carbonaceous materials
325 appears in both starting and functionalized samples, it is displayed at ≈ 1520 cm^{-1} and at 1560
326 cm^{-1} for the CNTs and the GNPs in Figs. 5a and 5b, respectively. The C-O and C=O signals
327 (expected from the grafted oxygen-containing groups) are observed for the samples oxidized
328 with the highest acid mixture concentrations, *i.e.* 5 and 7 M (NT-5M, NT-7M, G-5M, and G-
329 7M). Generally, for the CNTs, the absorption peaks observed at 1130 and 1230 cm^{-1} are
330 attributed to C-O stretching of carboxylic acid and alcohol groups, respectively. At the same
331 time the absorption peaks located between 1615 and 1790 cm^{-1}, characteristic of C=O
332 stretching, can be attributed to the presence of carboxylic acid and quinone groups [35,49–51].
333 For the GNP samples, the spectra present the characteristic signal of C-O stretching notably in
334 the 870-1275 cm^{-1} range and the presence of C=O, attributed to carboxylic specimens, at 1610
335 and 1760 cm^{-1} (Fig. 5b) [49,52]. Presence of oxygen containing groups for both MWCNTs
336 and GPNs is then clearly evidenced by FTIR. These results are in agreement with most of the
337 types of oxygen-containing functional group found by TG-MS (Table 2).

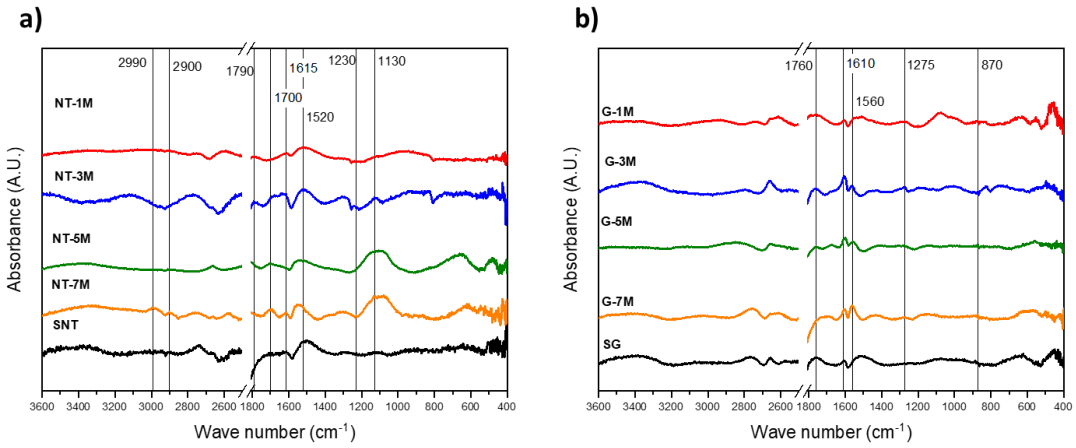

Figure 5 FTIR spectra of a) starting and treated MWCNTs by H_2SO_4/HNO_3 at 1, 3, 5 and 7 M (SNT, NT-1M, NT-3M, NT-5M and NT-7M) and b) starting and treated GNPs by H_2SO_4/HNO_3 at 1, 3, 5 and 7 M (SG, G-1M, G-3M, G-5M and G-7M).

The applied characterization analysis shows that oxidation was promoted in different proportion among both samples. Yet, it is evident that different degrees of structural damages may have occurred in the treated MWCNTs and GNPs. Besides, as reactivity differs among different nanocarbons depending on their amount of pre-existing defects [53], morphology, curvature [54], etc., MWCNT and GNP react differently to the same functionalization force making the compromise between dispersion ability and preservation of the intrinsic physical properties difficult to predict. In the following, both dispersion stability and TC measurements have been investigated to find the optimized degree of oxidation to apply in order to prepare efficient and stable nanofluids for heat transfer applications.

3.2 Thermal conductivity *vs.* stability of MWCNT and GNP based nanofluids

The TC of the prepared nanofluids, measured at 293.15 K (20 °C), are presented in Fig. 6 for MWCNT and GNP (Figs. 6a and 6b, respectively). The functionalized MWCNT- and GNP-based nanofluids present TC values higher than that of water as the base fluid. In both cases, significantly higher TC values are measured for the samples treated with the lowest acid

mixture concentration; *i.e.* at 1 M (NT-1M and G-1M). For MWCNTs (Fig. 6a), by taking into account the measurement uncertainty, TC remains in the same range around 0.65 $Wm^{-1}K^{-1}$ until the acid concentration of 5 M and TC diminishes significantly down to around 0.62 $Wm^{-1}K^{-1}$ for the sample treated with the acid mixture of concentration 7 M. This tendency is obviously observed for the calculated TC enhancements going from 9 % for samples NT-1M, NT-3M and NT-5M down to 4 % for NT-7M. For the GNP-based nanofluids, a similar behavior showing a decrease of the TC values (from 0.65 down to 0.61 $Wm^{-1}K^{-1}$) and enhancements (from 9 down to 3 %) is observed with a clear shift towards the lowest oxidative force. These results reveal a strong dependency between TC enhancements and the used H_2SO_4/HNO_3 concentration employed for chemical oxidation of the carbon nanomaterials. This dependency can be explained by the oxidation mechanism as it involves the disruption of the nanocarbons native structure as functionalization involves the attack and reaction of oxidants with the carbon-to-carbon bonds, causing sp^2 hybridized carbon atoms to break down into sp^3 carbon atoms. This process creates additional defects, facilitating the incorporation of functional groups onto the MWCNT and GNP surface and subsequently, increasing the defect populations leading to the loss of their intrinsic properties. This can explain why the extent of defect increment is linked to the acid concentration used during the functionalization process [35,55].

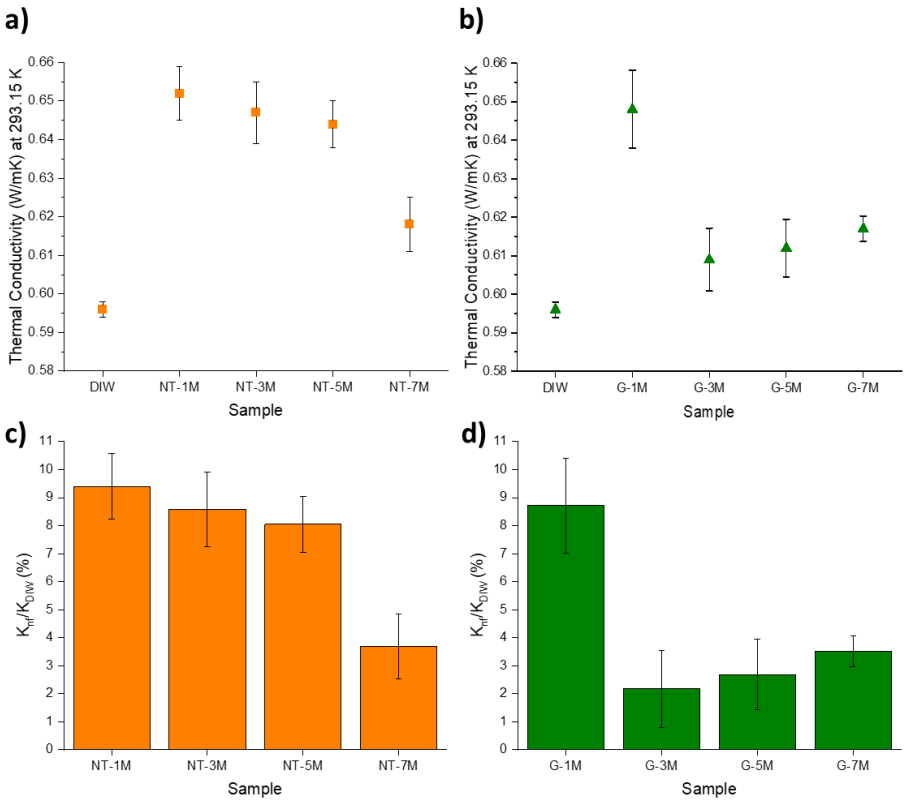

Figure 6 TC measurements of nanofluids (a and b) and TC enhancements (c and d) with respect to the base fluid prepared with a) and c) the treated MWCNTs by H_2SO_4/HNO_3 at 1, 3, 5 and 7 M (NT-1M, NT-3M, NT-5M and NT-7M) and b) and d) the treated GNPs by H_2SO_4/HNO_3 at 1, 3, 5 and 7 M (G-1M, G-3M, G-5M and G-7M).

The stability of the prepared nanofluids was further followed by means of UV-visible absorbance spectroscopy. According to the Beer-lambert law, a dispersion UV absorbance is proportional to its concentration. Normally, during destabilization, the carbon nanomaterials will aggregate slowly and sediment, leading to less particles being in suspension, therefore the higher the absorbance over time the better the stability [56]. Another commonly observed phenomenon for carbon nanomaterials leads to a slight increment of absorbance during dispersion settling. This behavior is consequence of nanocarbon flocculation-inducive attractive forces at the first stage of dispersion destabilization leading the nanoparticles to self-aggregate; these aggregates remaining in suspension for a while before the sedimentation

391 step [57,58]. The relative nanofluids absorbance during a 35 day-period is displayed in Figure
392 7. Contrasting behaviors can be observed between the oxidized MWCNT- and GNP- based
393 nanofluids (Figs. 7a and 7b, respectively). The nanofluids prepared with the MWCNTs
394 functionalized with H_2SO_4/HNO_3 at 7 M (NT-7M) remained stable after 35 days with a
395 relative increase in absorbance of 2 %. Likewise, nanofluids containing the MWCNTs treated
396 with an acidic mixture concentration at 3 and 5 M (NT-3M and NT-5M) show an absorbance
397 decrease of only 1 %. For the nanofluid prepared with the MWCNTs treated with the lowest
398 acid mixture concentration (NT-1M), a slight increase in absorbance (around 5 %) is observed
399 during the first 3 to 7 days and it presents a relative absorbance decrease of 20 % after the 35
400 days. As expected, the carbon nanomaterials treated with the highest functionalization rate
401 show a better endurance to sedimentation. For the GNP based nanofluids (Fig. 7b), an
402 important decay in the absorbance over time is rapidly seen since the early days of settling.
403 After 35 days, the nanofluids containing the GNPs treated with H_2SO_4/HNO_3 at 5 and 7 M
404 (G-5M and G-7M) present only 40 % of their initial relative absorbance. The GNP based
405 nanofluid treated with the 7 M acid mixture (G-7M) presents a small relative absorbance
406 increment during the first days similarly to what it was observed for sample NT-1M. The
407 relative absorbance drop becomes more pronounced for two nanofluids with the GNPs
408 functionalized with the lowest acid concentration (G-3M and G-1M) with a relative
409 absorbance of 30 and 20 %, respectively. Again here, the more oxidized the sample, the better
410 the stability improvement, being however not good for all the studied GNP based nanofluids.

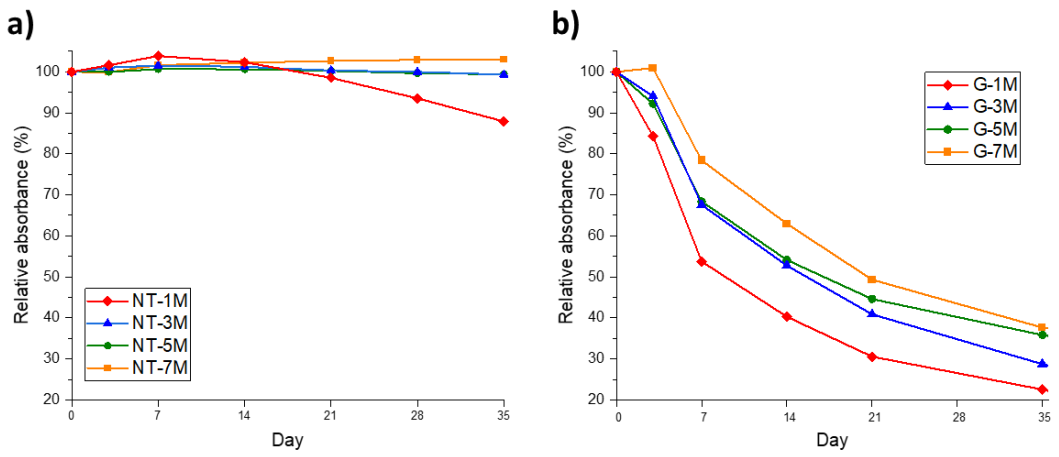

Figure 7 Relative absorbance over 35 days of the nanofluids (diluted 1:10) prepared with a) the treated MWCNTs by H_2SO_4/HNO_3 at 1, 3, 5 and 7 M (NT-1M, NT-3M, NT-5M and NT-7M) and b) the treated GNPs by H_2SO_4/HNO_3 at 1, 3, 5 and (7 M , G-1M, G-3M, G-5M and G-7M).

By observing TC and stability of the eight studied nanofluids (Figs. 6 and 7), it is clear that the MWCNTs oxidized with H_2SO_4/HNO_3 at 3 and 5 M concentrations (NT-3M and NT-5M respectively) present the best compromise between the nanofluids two main requirements. This compromise for the MWCNTs cannot be achieved with the GNPs showing a lack of stability for all the used conditions for the applied chemical modification. As it was stated before, the different reactivity between MWCNT and GNP would result in different nanofluid performances. Furthermore, even if the functionalization seems efficient on GNP (significant increase in I_D/I_G), the functionalization level seems not sufficient to counterbalance the aggregation forces, explaining the poor stability of the oxidized GNPs, even at the highest used acid mixture concentration (G-7M). Possibly for the GNP, the TC enhancement window and the carbon structure damaging do not concur, making impossible to find the desired compromise for this kind of carbon nanomaterial and this kind of functionalization approach.

Evolution of the nanofluids TC increment as a function of the I_D/I_G which is sensitive to damaging (amount of defects) of the chemically modified MWCNTs and GNPs is shown in

Figs. 8a and 8b, respectively (the gray plotted line serves as a visual guide). For the oxidized MWCNTs, as the number of defects increases in the carbon network due to the strength of the oxidation treatment, the TC increment is roughly maintained with a slight decrease and drops rapidly above a certain degree of defects introduced in the carbon nanomaterials. From the results obtained above, the I_D/I_G range where the carbon nanomaterial dispersion is stable is displayed as visual guidance (in blue). Remarkably is the fact that the TC increment drop is not located at the beginning of the stable dispersion zone, suggesting that samples located in between (NT-3M and NT-5M) are capable to fulfill both stability and TC requirements for the prepared nanofluid. For the oxidized GNPs, a similar TC increment drop is observed but with a strongest sensitivity to the oxidation treatment conditions (Fig. 8b). Contrary to a continuous process, the observed interplay between TC enhancement and defect amount in the carbon network suggests the existence of a threshold above which the phonon pathway is broken and beyond which TC suddenly drops. This finding evidences the best compromise to be found by maximizing the sample stability and at the same time limiting the carbon structure damaged by the chemical treatments.

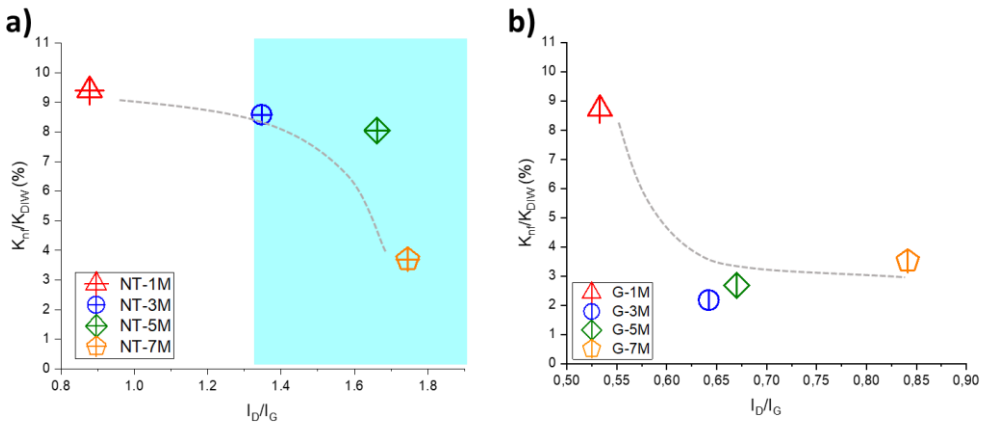

Figure 8 Nanofluid TC increment *vs.* Raman spectroscopy I_D/I_G values of a) the treated MWCNTs by H_2SO_4/HNO_3 at 1, 3, 5 and 7 M (NT-1M, NT-3M, NT-5M and NT-7M) and b) the treated GNPs by H_2SO_4/HNO_3 at 1, 3, 5 and 7 M (G-1M, G-3M, G-5M and G-7M).

3.3 Thermal conductivity performances of the prepared MWCNT and GNP nanofluids

With the aim to compare the efficiency between the nanofluids prepared here with oxidized MWCNTs and GNPs, a TC performance parameter, namely P_{TC}, derivative from Pavía *et al.* [31] is considered. This parameter allows to compare the efficiency of nanofluids prepared with different nanoparticles by considering the nanofluid TC enhancement divided by the amount of the employed nanomaterial used to prepare the nanofluid. In this work, the P_{TC} parameter is calculated with the TC enhancement reported at 20 °C and divided by temperature (in °C) as described in Eq.1:

$$P_{TC} = \frac{TC_e}{C_{NP}.T_m} \qquad \text{(Eq.1)}$$

where TC_e is the measured thermal conductivity enhancement with respect to the base fluid at 20 °C, C_{NP} is the nanoparticle concentration (wt. %) of the employed nanocarbon and T_m is the temperature (°C) of the TC measurements [31].

Initially, the P_{TC} was calculated applying Eq. 1 for the 8 prepared nanofluids. The results are gathered in Table 3 below.

Table 3 Functionalized MWCNT- and GNP-based nanofluid preparation conditions, TC enhancements with respect to base fluid and the calculated TC parameter, P_{TC} .

Functionalization method conditions	**Sample**	**Thermal conductivity**	
		TC enhancement	**P_{TC} (% increment/ wt. % per °C)**
300 mL H_2SO_4:HNO_3, 1:1 v/v at 1 M reflux during 24 h	NT-1M	9.4	1.88
	G-1M	8.72	1.74
300 mL H_2SO_4:HNO_3, 1:1 v/v	NT-3M	8.58	1.72

at 3 M reflux during 24 h	G-3M	2.18	0.44
300 mL H_2SO_4:HNO_3, 1:1 v/v at 5 M reflux during 24 h	NT-5M	8.05	1.61
	G-5M	2.68	0.54
300 mL H_2SO_4:HNO_3, 1:1 v/v at 7 M reflux during 24 h	NT-7M	3.69	0.74
	G-7M	3.52	0.70

469

470 P_{TC} values obtained for the two nanocarbons treated with the lowest functionalization force
471 (H_2SO_4/HNO_3 at 1 M) are in the same range (Table 3). However, as the acid concentration
472 increases, a different impact on MWCNT and GNP TC performances appears. With G-3M
473 and G-5M, P_{TC} values were less than half of those obtained for MWCNTs at same treatment.
474 At 7 M, similar values of P_{TC} were found for both oxidized MWCNTs and GNPs (NT-7M and
475 G-7M).

476 As the treated MWCNT based nanofluids in this study exhibited superior stability over time
477 and TC performances (TC enhancement and P_{TC}), they were compared with analogous
478 samples treated under similar conditions, *i.e.* acid treated MWCNTs whose TC is reported in
479 literature Previous works used for comparison purpose are gathered in Table 4. The CNT
480 concentration influence in the nanofluid TC enhancement not always result in high P_{TC} values
481 as already been discussed in literature [31]. Additionally, nanofluids prepared with oxidized
482 MWCNTs by the acid mixture of H_2SO_4 and HNO_3 in literature present a P_{TC} (% of TC
483 increment per wt.% of CNT per °C) in the 0.3-7 range. From a detailed analysis of Table 4, it
484 could be inferred that oxidizing MWCNTs by the H_2SO_4/HNO_3 mixture results, in general, in
485 CNTs with good thermal properties that are later reflected in good nanofluids TC
486 enhancements. By comparing the applied functionalization methods, it seems that oxidizing
487 the CNTs with mild conditions (relatively low acid concentrations, shortest stirring/refluxing
488 times, etc.) does not necessarily result in high P_{TC} values (and neither for strong conditions, as

489 expected). Interestingly, for some nanofluids prepared under practically the same
490 circumstances and with similar MWCNT concentrations, contrasting P_{TC} values were found.
491 In the works of Ghozatloo *et al.* [42] and Van Trinh *et al.* [59], P_{TC} values of 6.73 and 0.21
492 are obtained, respectively. Such difference might arise from the variance among the used
493 starting MWCNT geometrical characteristics and/or the preexisting defect amount that will
494 influence the functionalization degree and the CNT network disruption of the outcoming
495 species and eventually their impact on the nanofluid TC.

496 Different techniques can be used to evaluate nanofluid stability, being the most recurrent the
497 direct visual observation, UV-visible and Zeta potential. The first method is well known as a
498 purely qualitative analysis, while the last two offer a more trustful and quantitative inquiry.
499 Zeta potential measures the surface charge around the dispersed nanomaterial giving an idea
500 of the stability of colloidal dispersions at a given time. UV-visible spectroscopy performed
501 over time can provide quantitative data about nanofluid stability during long time periods. As
502 it was stated before, nanofluids must remain stable for being efficiently used as heat transfer
503 fluids in cooling systems. Stability of nanofluids over time investigated by UV-visible
504 spectroscopy was performed only in half the works gathered in Table 4, including the
505 nanofluids prepared in this article. Good stability over time has been successfully reported for
506 80 days by Farbod *et al.* [60] while Ghozatloo *et al.* [42] have followed their MWCNT based
507 nanofluid stability only during 800 min. In the work by Hussein *et al.* [61], stability is
508 mentioned to be investigated by UV-visible spectroscopy however, no clear data are given
509 over time. For the other works, only visual observations and Zeta potential measurements
510 were performed forbidding stability over time studies. The analysis of P_{TC}/nanofluid stability
511 relationship for the best P_{TC} calculated for each reported work is provided below. P_{TC} is found
512 to be quite high (6.73 % TC increment / wt. % per °C) for the MWCNT based nanofluids
513 prepared by Ghozatloo *et al.* [42] but with the nanofluid stability only followed over 800 min.

514 For the other reported highest P_{TC} values (5.87 and 5.36 TC increment / wt. % per °C from
515 refs. [61] and [62], respectively) with no investigation of the stability of the corresponding
516 prepared nanofluids. P_{TC} are found quite low (0.34 and 0.37 TC increment / wt. % per °C
517 from refs. [59] and [63], respectively). The performances of the nanofluids prepared by
518 Farbod *et al.* [60] with MWCNTs oxidized with a H_2SO_4/HNO_3 mixture show a good
519 dispersion stability over 80 days (absorption decay of 10 %) and a P_{TC} of 3 TC increment /
520 wt. % per °C which is close to the best value found in this work.

521 The P_{TC}/stability compromise found in this study for the nanofluids containing treated
522 MWCNTs is better for the MWCNTs oxidized with intermediate functionalization forces, *i.e.*
523 3 M and 5 M (NT-3M and NT-5M) among the investigated acid mixture concentration range.
524 Furthermore, the stability evaluation displays that the nanofluids prepared with NT-3M and
525 NT-5M remained stable for at least 5 weeks suggesting that both important nanofluids criteria
526 were achieved.

527 **Table 4** Functionalized MWCNT-based nanofluid preparation conditions, including MWCNT source, functionalization treatment, nanoparticle
528 concentration, temperature used to measure TC, TC enhancement with respect to base fluid, calculated TC parameter (P_{TC}) and stability
529 investigation including the used technique and the found stability time.

Sample nature	**Functionalization method conditions**	**CNT conc. (wt. %)**	**Thermal conductivity measurements**				**Stability measurements**		**Ref**
			T (°C)	**TC (W/mK)**	**TC enhancement**	**P_{TC} (% increment/ wt. % per °C**	**Measurement technique**	**Measurement over time**	
MWCNTs	300 mL H_2SO_4:HNO_3, 1:1 v/v at 1 M reflux during 24 h	0.25	RT	0.65	9.4	1.88	UV-visible absorption	35 days. Sample max. absorbance decay 20%	This work
MWCNTs	300 mL H_2SO_4:HNO_3, 1:1 v/v at 3 M reflux during 24 h	0.25	RT	0.64	8.58	1.72	UV-visible absorption	35 days. Sample stable, no absorbance	This work

								decay.	
MWCNTs	300 mL H_2SO_4:HNO_3, 1:1 v/v at 5 M reflux during 24 h	0.25	RT	0.64	8.05	1.61	UV-visible absorption	35 days. Sample stable, no absorbance decay.	This work
MWCNTs	300 mL H_2SO_4:HNO_3, 1:1 v/v at 7 M reflux during 24 h	0.25	RT	0.62	3.69	0.74	UV-visible absorption	35 days. Sample stable, no absorbance decay.	This work
MWCNT commercial	40 ml of pure HNO_3 reflux during 1 h	0.4	RT	N.A.	3	0.37	Direct visual observation	2 months, no visible precipitation	[63]
MWCNT commercial	Pure H_2SO_4:HNO_3, 3:1 v/v sonicated during 30 min and reflux during 4 h	0.1	40	0.61	12	3	UV-visible absorption	80 days. Sample absorbance decay 10%	[60]

MWCNT commercial	Pure H_2SO_4:HNO_3, 3:1 v/v sonicated during 30 min and reflux during 4 h	0.25	40	0.59	10	1	UV-visible absorption	80 days. Sample absorbance decay 20%	[60]
MWCNT commercial	Pure H_2SO_4:HNO_3, 3:1 v/v sonicated during 30 min and reflux during 4 h	0.5	40	0.63	11	0.55	UV-visible absorption	80 days. Sample absorbance decay 30%	[60]
MWCNT commercial	40 ml Pure H_2SO_4:HNO_3, 3:1 v/v and reflux during 1 h	0.1	RT	0.66	10.73	5.36	Direct visual observation	N.A.	[62]
MWCNT commercial	40 ml Pure H_2SO_4:HNO_3, 3:1 v/v and reflux during 1 h	0.05	RT	0.61	2.34	2.34	Direct visual observation	N.A.	[62]
MWCNT commerci	Pure H_2SO_4:HNO_3, 3:1 v/v stirring 1h and then	0.02	RT	0.61	2.34	5.87	UV-visible absorption	N.A	[61]

al	sonication bath during 3 h								
MWCNT commercial	Pure H_2SO_4:HNO_3, 3:1 v/v stirring 1h and then sonication bath during 3 h	0.05	RT	0.63	1.05	1.05	UV-visible absorption	N.A.	[61]
MWCNT commercial	Pure H_2SO_4:HNO_3, 3:1 v/v stirring 1h and then sonication bath during 3 h	0.08	RT	0.65	9.06	5.66	UV-visible absorption	N.A.	[61]
MWCNT commercial	Pure H_2SO_4:HNO_3, 3:1 v/v stirring 1h and then sonication bath during 3 h	0.1	RT	0.66	10.73	5.36	UV-visible absorption	N.A.	[61]
MWCNT commerci	Pure H_2SO_4:HNO_3, 3:1 v/v stirring for 100 min	0.1	25	0.71	16.83	6.73	UV-Visible transmittance	800 min. Transmittance	[42]

al								increment of 0.5 %	
MWCNT by CVD	Pure H_2SO_4:HNO_3, 3:1 v/v stirring for 3 h	0.16	30	0.61	1	0.21	Zeta potential	N.A.	[59]
MWCNT by CVD	Pure H_2SO_4:HNO_3, 3:1 v/v stirring for 5 h	0.16	30	0.62	1.65	0.34	Zeta potential	N.A.	[59]
MWCNT by CVD	Pure H_2SO_4:HNO_3, 3:1 v/v stirring for 7 h	0.16	30	0.61	1.16	0.24	Zeta potential	N.A.	[59]

530

531

Conclusion

MWCNTs and GNPs have been submitted to a functionalization treatment under H_2SO_4/HNO_3 mixture with a gradual increase in concentration modifying that way the oxidation power applied. The chemically modified MWCNTs and GNPs have been investigated by means of several characterization methods so that the amount of defects/functional groups in the carbon framework was followed upon the applied chemical treatments. The thermal conductivity of nanofluids produced with those MWCNTs and GNPs is put into perspective with the carbon nanomaterial damage and the nanofluid stability studied during 35 days by means of UV-visible spectroscopy. It appears that the GNP-based nanofluids suffer from a lack of stability even for the highest functionalized rate making unreachable a good compromise between TC preservation and structural damaging by the applied chemical functionalization treatment. For the MWCNT-based nanofluids, an interesting compromise can be found. It allows i) limiting the amount of structural defects introduced by the chemical treatment and consequently the decrease in nanofluid thermal conductivity and ii) a remarkable stability of the oxidized MWCNT based nanofluids is observed (without addition of surfactant). The difference between the GNP and MWCNT performance presumably originates from different reactivity towards the oxidative force, suggesting the existence of a limit for each material after which the defect introduction causes a change in both stability and thermal conductivity of carbon-based nanofluids. As rarely reported, this work provides the study of a coupled effect between the chemical treatment applied to the carbon nanomaterial, the nanofluid stability and the TC performance. Such strategy, tuning the functionalization strength allowing to optimize nanofluid TC *vs.* stability, could be used for other functionalization treatments with the purpose of searching to maximize TC even more while keeping a good stability. From such a compromise, it would be interesting to apply the proposed approach to any carbon nanomaterials such as

nanodiamonds, nanofibers… and to move the focus towards the diminution of the nanomaterial concentration. We strongly believe that such investigation will lead to more research evaluating the carbon-based nanofluid stability over time in regards with TC measurements which would offer a crucial step towards nanofluids for more realistic performance evaluation.

Author Contributions

Experiments, methodology, nanofluid preparation, spectroscopy characterization, writing and data analysis: M.P.; TEM imaging and analysis: M.E.; thermal conductivity, data analysis, writing, review and editing: P.E. MWCNT synthesis supervision, project administration and funding acquisition: A.R.M.; supervision project administration, funding acquisition, data analyzing, methodology, writing, review and editing: B.V.

Acknowledgments

The authors are grateful to IDEX/I-SITE and the Lorraine Université d'Excellence (LUE) for the funding of this work. The authors would like to thank the platforms "Microscopies, Microprobes and Metallography (3M)", "X-Gamma", "Optics and Laser" and "Magnetism and Cryogenics" (Institut Jean Lamour, IJL, Nancy, France) for facilities access, Jaafar Ghanbaja and Sébastien Hupont for their valuable help for TEM and UV-Visible spectroscopy experiments, respectively , Lionel Aranda for his help during TGA experiments and Soulayma Gal for assistance in TC evaluation.

Conflicts of interest

The authors are no conflicts to declare.

References

[1] S.U.S. Choi, J.A. Eastman, Enhacing thermal conductivity of fluids with nanoparticles, in: 1995: p. 8.

[2] A. Kumar, S. Subudhi, Nanofluids: Definition & Classification, in: Thermal Characteristics and Convection in Nanofluids, Springer Singapore, Singapore, 2021: pp. 11–24. https://doi.org/10.1007/978-981-33-4248-4_2.

[3] J. Patel, A. Soni, D.P. Barai, B.A. Bhanvase, A minireview on nanofluids for automotive applications: Current status and future perspectives, Applied Thermal Engineering. 219 (2023) 119428. https://doi.org/10.1016/j.applthermaleng.2022.119428.

[4] A.H. Elsheikh, S.W. Sharshir, M.E. Mostafa, F.A. Essa, M.K. Ahmed Ali, Applications of nanofluids in solar energy: A review of recent advances, Renewable and Sustainable Energy Reviews. 82 (2018) 3483–3502. https://doi.org/10.1016/j.rser.2017.10.108.

[5] Z. Said, L.S. Sundar, A.K. Tiwari, H.M. Ali, M. Sheikholeslami, E. Bellos, H. Babar, Recent advances on the fundamental physical phenomena behind stability, dynamic motion, thermophysical properties, heat transport, applications, and challenges of nanofluids, Physics Reports. 946 (2022) 1–94. https://doi.org/10.1016/j.physrep.2021.07.002.

[6] L. Qiu, N. Zhu, Y. Feng, E.E. Michaelides, G. Żyła, D. Jing, X. Zhang, P.M. Norris, C.N. Markides, O. Mahian, A review of recent advances in thermophysical properties at the nanoscale: From solid state to colloids, Physics Reports. 843 (2020) 1–81. https://doi.org/10.1016/j.physrep.2019.12.001.

[7] H. Malekpour, P. Ramnani, S. Srinivasan, G. Balasubramanian, D.L. Nika, A. Mulchandani, R.K. Lake, A.A. Balandin, Thermal conductivity of graphene with defects induced by electron beam irradiation, Nanoscale. 8 (2016) 14608–14616. https://doi.org/10.1039/C6NR03470E.

[8] A. Samadzadeh, S. Zeinali Heris, Effect of stabilization method on the natural convection in an inclined cavity filled with MWCNTs/water nanofluids, International Communications in Heat and Mass Transfer. 129 (2021) 105645. https://doi.org/10.1016/j.icheatmasstransfer.2021.105645.

[9] Z. Mingzheng, X. Guodong, L. Jian, C. Lei, Z. Lijun, Analysis of factors influencing thermal conductivity and viscosity in different kinds of surfactant solutions, Experimental Thermal and Fluid Science. 36 (2012) 22–29. https://doi.org/10.1016/j.expthermflusci.2011.07.014.

[10] O.A. Hussein, K. Habib, R. Saidur, A.S. Muhsan, S. Shahabuddin, O.A. Alawi, The influence of covalent and non-covalent functionalization of GNP based nanofluids on its thermophysical, rheological and suspension stability properties, RSC Adv. 9 (2019) 38576–38589. https://doi.org/10.1039/C9RA07811H.

[11] A.K. Geim, K.S. Novoselov, The rise of graphene, Nature Mater. 6 (2007) 183–191. https://doi.org/10.1038/nmat1849.

[12] S. Rathinavel, K. Priyadharshini, D. Panda, A review on carbon nanotube: An overview of synthesis, properties, functionalization, characterization, and the application, Materials Science and Engineering: B. 268 (2021) 115095. https://doi.org/10.1016/j.mseb.2021.115095.

[13] N. Gupta, S.M. Gupta, S.K. Sharma, Carbon nanotubes: synthesis, properties and engineering applications, Carbon Lett. 29 (2019) 419–447. https://doi.org/10.1007/s42823-019-00068-2.

[14] C. Backes, A.M. Abdelkader, C. Alonso, A. Andrieux-Ledier, R. Arenal, J. Azpeitia, N. Balakrishnan, L. Banszerus, J. Barjon, R. Bartali, S. Bellani, C. Berger, R. Berger, M.M.B. Ortega, C. Bernard, P.H. Beton, A. Beyer, A. Bianco, P. Boggild, F. Bonaccorso, G.B. Barin, C. Botas, R.A. Bueno, D. Carriazo, A. Castellanos-Gomez, M. Christian, A. Ciesielski, T. Ciuk, M.T. Cole, J. Coleman, C. Coletti, L. Crema, H. Cun, D. Dasler, D. De Fazio, N. Diez, S. Drieschner, G.S. Duesberg, R. Fasel, X. Feng, A. Fina, S. Forti, C. Galiotis, G. Garberoglio, J.M. Garcia, J. Antonio Garrido, M. Gibertini, A. Goelzhaeuser, J. Gomez, T. Greber, F. Hauke, A. Hemmi, I. Hernandez-Rodriguez, A. Hirsch, S.A. Hodge, Y. Huttel, P.U. Jepsen, I. Jimenez, U. Kaiser, T. Kaplas, H. Kim, A. Kis, K. Papagelis, K. Kostarelos, A. Krajewska, K. Lee, C. Li, H. Lipsanen, A. Liscio, M.R. Lohe, A. Loiseau, L. Lombardi, M. Francisca Lopez, O. Martin, C. Martin, L. Martinez, J. Angel Martin-Gago, J. Ignacio Martinez,

N. Marzari, A. Mayoral, J. McManus, M. Melucci, J. Mendez, C. Merino, P. Merino, A.P. Meyer, E. Miniussi, V. Miseikis, N. Mishra, V. Morandi, C. Munuera, R. Munoz, H. Nolan, L. Ortolani, A.K. Ott, I. Palacio, V. Palermo, J. Parthenios, I. Pasternak, A. Patane, M. Prato, H. Prevost, V. Prudkovskiy, N. Pugno, T. Rojo, A. Rossi, P. Ruffieux, P. Samori, L. Schue, E. Setijadi, T. Seyller, G. Speranza, C. Stampfer, I. Stenger, W. Strupinski, Y. Svirko, S. Taioli, K.B.K. Teo, M. Testi, F. Tomarchio, M. Tortello, E. Treossi, A. Turchanin, E. Vazquez, E. Villaro, P.R. Whelan, Z. Xia, R. Yakimova, S. Yang, G. Reza Yazdi, C. Yim, D. Yoon, X. Zhang, X. Zhuang, L. Colombo, A.C. Ferrari, M. Garcia-Hernandez, Production and processing of graphene and related materials, 2D Mater. 7 (2020) 022001. https://doi.org/10.1088/2053-1583/ab1e0a.

[15] X.-K. Chen, K.-Q. Chen, Thermal transport of carbon nanomaterials, J. Phys.: Condens. Matter. 32 (2020) 153002. https://doi.org/10.1088/1361-648X/ab5e57.

[16] A. Arshad, M. Jabbal, Y. Yan, D. Reay, A Review on Graphene based Nanofluids: Preparation, Characterization and Applications, Journal of Molecular Liquids. 279 (2019) 444–484. https://doi.org/10.1016/j.molliq.2019.01.153.

[17] M. Ghalandari, A. Maleki, A. Haghighi, M. Safdari Shadloo, M. Alhuyi Nazari, I. Tlili, Applications of nanofluids containing carbon nanotubes in solar energy systems: A review, Journal of Molecular Liquids. 313 (2020) 113476. https://doi.org/10.1016/j.molliq.2020.113476.

[18] A. Banisharif, P. Estellé, A. Rashidi, S. Van Vaerenbergh, M. Aghajani, Heat transfer properties of metal, metal oxides, and carbon water-based nanofluids in the ethanol condensation process, Colloids and Surfaces A: Physicochemical and Engineering Aspects. 622 (2021) 126720. https://doi.org/10.1016/j.colsurfa.2021.126720.

[19] P. Yadav, S.M. Gupta, S.K. Sharma, A review on stabilization of carbon nanotube nanofluid, J Therm Anal Calorim. 147 (2022) 6537–6561. https://doi.org/10.1007/s10973-021-10999-6.

[20] N. Trong Tam, N. Viet Phuong, P. Hong Khoi, P. Ngoc Minh, M. Afrand, P. Van Trinh, B. Hung Thang, G. Żyła, P. Estellé, Carbon Nanomaterial-Based Nanofluids for Direct Thermal Solar Absorption, Nanomaterials. 10 (2020) 1199. https://doi.org/10.3390/nano10061199.

[21] A. Amiri, M. Shanbedi, M.J. AliAkbarzade, The Specific Heat Capacity, Effective Thermal Conductivity, Density, and Viscosity of Coolants Containing Carboxylic Acid Functionalized Multi-Walled Carbon Nanotubes, Journal of Dispersion Science and Technology. 37 (2016) 949–955. https://doi.org/10.1080/01932691.2015.1074588.

[22] S. Hamze, D. Cabaleiro, P. Estellé, Graphene-based nanofluids: A comprehensive review about rheological behavior and dynamic viscosity, Journal of Molecular Liquids. 325 (2021) 115207. https://doi.org/10.1016/j.molliq.2020.115207.

[23] P. Estellé, S. Halelfadl, T. Maré, Lignin as dispersant for water-based carbon nanotubes nanofluids: Impact on viscosity and thermal conductivity, International Communications in Heat and Mass Transfer. 57 (2014) 8–12. https://doi.org/10.1016/j.icheatmasstransfer.2014.07.012.

[24] E. Voss, Covalent functionalization of polyhedral graphitic particles synthesized by arc discharge from graphite, (2017) 6.

[25] A. Chouhan, H.P. Mungse, O.P. Khatri, Surface chemistry of graphene and graphene oxide: A versatile route for their dispersion and tribological applications, Advances in Colloid and Interface Science. 283 (2020) 102215. https://doi.org/10.1016/j.cis.2020.102215.

[26] M. Shanbedi, S.Z. Heris, A. Amiri, H. Eshghi, Synthesis of water-soluble Fe-decorated multi-walled carbon nanotubes: A study on thermo-physical properties of ferromagnetic nanofluid, Journal of the Taiwan Institute of Chemical Engineers. 60 (2016) 547–554. https://doi.org/10.1016/j.jtice.2015.10.008.

[27] M. Shanbedi, S.Z. Heris, A. Amiri, E. Hosseinipour, H. Eshghi, S.N. Kazi, Synthesis of aspartic acid-treated multi-walled carbon nanotubes based water coolant and experimental investigation of thermal and hydrodynamic properties in circular tube, Energy Conversion and Management. 105 (2015) 1366–1376. https://doi.org/10.1016/j.enconman.2015.09.002.

[28] D. Cabaleiro, L. Colla, S. Barison, L. Lugo, L. Fedele, S. Bobbo, Heat Transfer Capability of (Ethylene Glycol + Water)-Based Nanofluids Containing Graphene Nanoplatelets: Design and

Thermophysical Profile, Nanoscale Res Lett. 12 (2017) 53. https://doi.org/10.1186/s11671-016-1806-x.
[29] K.A. Wepasnick, B.A. Smith, K.E. Schrote, H.K. Wilson, S.R. Diegelmann, D.H. Fairbrother, Surface and structural characterization of multi-walled carbon nanotubes following different oxidative treatments, Carbon. 49 (2011) 24–36. https://doi.org/10.1016/j.carbon.2010.08.034.
[30] G. Yang, L. Li, W.B. Lee, M.C. Ng, Structure of graphene and its disorders: a review, Science and Technology of Advanced Materials. 19 (2018) 613–648. https://doi.org/10.1080/14686996.2018.1494493.
[31] M. Pavía, K. Alajami, P. Estellé, A. Desforges, B. Vigolo, A critical review on thermal conductivity enhancement of graphene-based nanofluids, Advances in Colloid and Interface Science. (2021) 17.
[32] T. Le Ba, O. Mahian, S. Wongwises, I.M. Szilágyi, Review on the recent progress in the preparation and stability of graphene-based nanofluids, J Therm Anal Calorim. 142 (2020) 1145–1172. https://doi.org/10.1007/s10973-020-09365-9.
[33] R.M. Firdaus, N.I.M. Rosli, J. Ghanbaja, B. Vigolo, A.R. Mohamed, Enhanced adsorption of methylene blue on chemically modified graphene nanoplatelets thanks to favorable interactions, J Nanopart Res. 21 (2019) 257. https://doi.org/10.1007/s11051-019-4701-4.
[34] L. Thi Mai Hoa, Characterization of multi-walled carbon nanotubes functionalized by a mixture of HNO3/H2SO4, Diamond and Related Materials. 89 (2018) 43–51. https://doi.org/10.1016/j.diamond.2018.08.008.
[35] W.-C. Teoh, W.-M. Yeoh, A.R. Mohamed, Evaluation of Different Oxidizing Agents on Effective Covalent Functionalization of Multiwalled Carbon Nanotubes, Fuller. Nanotub. Carbon Nanostruct. 26 (2018) 846–850. https://doi.org/10.1080/1536383X.2018.1508133.
[36] W.-M. Yeoh, K.-Y. Lee, S.-P. Chai, K.-T. Lee, A.R. Mohamed, Synthesis of high purity multi-walled carbon nanotubes over Co-Mo/MgO catalyst by the catalytic chemical vapor deposition of methane, New Carbon Materials. 24 (2009) 119–123. https://doi.org/10.1016/S1872-5805(08)60041-4.
[37] T. Bortolamiol, P. Lukanov, A.-M. Galibert, B. Soula, P. Lonchambon, L. Datas, E. Flahaut, Double-walled carbon nanotubes: Quantitative purification assessment, balance between purification and degradation and solution filling as an evidence of opening, Carbon. 78 (2014) 79–90. https://doi.org/10.1016/j.carbon.2014.06.051.
[38] S. Hamze, N. Berrada, D. Cabaleiro, A. Desforges, J. Ghanbaja, J. Gleize, D. Bégin, F. Michaux, T. Maré, B. Vigolo, P. Estellé, Few-Layer Graphene-Based Nanofluids with Enhanced Thermal Conductivity, Nanomaterials. 10 (2020) 1258. https://doi.org/10.3390/nano10071258.
[39] J.I. Prado, U. Calviño, L. Lugo, Experimental Methodology to Determine Thermal Conductivity of Nanofluids by Using a Commercial Transient Hot-Wire Device, Applied Sciences. 12 (2021) 329. https://doi.org/10.3390/app12010329.
[40] R. Sadri, M. Hosseini, S.N. Kazi, S. Bagheri, S.M. Ahmed, G. Ahmadi, N. Zubir, M. Sayuti, M. Dahari, Study of environmentally friendly and facile functionalization of graphene nanoplatelet and its application in convective heat transfer, Energy Conversion and Management. 150 (2017) 26–36. https://doi.org/10.1016/j.enconman.2017.07.036.
[41] M. Mehrali, E. Sadeghinezhad, S. Latibari, S. Kazi, M. Mehrali, M.N.B.M. Zubir, H.S. Metselaar, Investigation of thermal conductivity and rheological properties of nanofluids containing graphene nanoplatelets, Nanoscale Res Lett. 9 (2014) 15. https://doi.org/10.1186/1556-276X-9-15.
[42] A. Ghozatloo, A.M. Rashidi, M. Shariaty-Niasar, Effects of surface modification on the dispersion and thermal conductivity of CNT/water nanofluids, International Communications in Heat and Mass Transfer. 54 (2014) 1–7. https://doi.org/10.1016/j.icheatmasstransfer.2014.02.013.
[43] R. Rastogi, R. Kaushal, S.K. Tripathi, A.L. Sharma, I. Kaur, L.M. Bharadwaj, Comparative study of carbon nanotube dispersion using surfactants, Journal of Colloid and Interface Science. 328 (2008) 421–428. https://doi.org/10.1016/j.jcis.2008.09.015.

[44] K. Raiah, A. Djalab, A. Hadj-Ziane-Zafour, B. Soula, A.-M. Galibert, E. Flahaut, Influence of the hydrocarbon chain length of imidazolium-based ionic liquid on the dispersion and stabilization of double-walled carbon nanotubes in water, Colloids and Surfaces A: Physicochemical and Engineering Aspects. 469 (2015) 107–116. https://doi.org/10.1016/j.colsurfa.2015.01.015.
[45] V. Datsyuk, M. Kalyva, K. Papagelis, J. Parthenios, D. Tasis, A. Siokou, I. Kallitsis, C. Galiotis, Chemical oxidation of multiwalled carbon nanotubes, Carbon. 46 (2008) 833–840. https://doi.org/10.1016/j.carbon.2008.02.012.
[46] S. Osswald, E. Flahaut, H. Ye, Y. Gogotsi, Elimination of D-band in Raman spectra of double-wall carbon nanotubes by oxidation, Chemical Physics Letters. 402 (2005) 422–427. https://doi.org/10.1016/j.cplett.2004.12.066.
[47] M.S. Dresselhaus, G. Dresselhaus, R. Saito, A. Jorio, Raman spectroscopy of carbon nanotubes, Physics Reports. 409 (2005) 47–99. https://doi.org/10.1016/j.physrep.2004.10.006.
[48] J.L. Figueiredo, M.F.R. Pereira, M.M.A. Freitas, J.J.M. Orfao, Modification of the surface chemistry of activated carbons, Carbon. 37 (1999) 1379–1389. https://doi.org/10.1016/S0008-6223(98)00333-9.
[49] V.A. Chhabra, A. Deep, R. Kaur, R. Kumar, Functionalization of Graphene using Carboxylation process, (2012).
[50] H. Peng, L.B. Alemany, J.L. Margrave, V.N. Khabashesku, Sidewall Carboxylic Acid Functionalization of Single-Walled Carbon Nanotubes, J. Am. Chem. Soc. 125 (2003) 15174–15182. https://doi.org/10.1021/ja037746s.
[51] G. Ovejero, J.L. Sotelo, M.D. Romero, A. Rodríguez, M.A. Ocaña, G. Rodríguez, J. García, Multiwalled Carbon Nanotubes for Liquid-Phase Oxidation. Functionalization, Characterization, and Catalytic Activity, Ind. Eng. Chem. Res. 45 (2006) 2206–2212. https://doi.org/10.1021/ie051079p.
[52] V. Ţucureanu, A. Matei, A.M. Avram, FTIR Spectroscopy for Carbon Family Study, Critical Reviews in Analytical Chemistry. 46 (2016) 502–520. https://doi.org/10.1080/10408347.2016.1157013.
[53] A.J. Clancy, H. Au, N. Rubio, G.O. Coulter, M.S.P. Shaffer, Understanding and controlling the covalent functionalisation of graphene, Dalton Trans. 49 (2020) 10308–10318. https://doi.org/10.1039/D0DT01589J.
[54] S. Park, D. Srivastava, K. Cho, Generalized Chemical Reactivity of Curved Surfaces: Carbon Nanotubes, Nano Lett. 3 (2003) 1273–1277. https://doi.org/10.1021/nl0342747.
[55] J. Chen, L. Li, Effect of oxidation degree on the thermal properties of graphene oxide, Journal of Materials Research and Technology. 9 (2020) 13740–13748. https://doi.org/10.1016/j.jmrt.2020.09.092.
[56] B. Wang, R. Jiang, W. Song, H. Liu, Controlling dispersion of graphene nanoplatelets in aqueous solution by ultrasonic technique, Russ. J. Phys. Chem. 91 (2017) 1517–1526. https://doi.org/10.1134/S0036024417080040.
[57] A.J. Blanch, C.E. Lenehan, J.S. Quinton, Optimizing Surfactant Concentrations for Dispersion of Single-Walled Carbon Nanotubes in Aqueous Solution, J. Phys. Chem. B. 114 (2010) 9805–9811. https://doi.org/10.1021/jp104113d.
[58] F. Zhang, D.G. Dressen, M.W.A. Skoda, R.M.J. Jacobs, S. Zorn, R.A. Martin, C.M. Martin, G.F. Clark, F. Schreiber, Gold nanoparticles decorated with oligo(ethylene glycol) thiols: kinetics of colloid aggregation driven by depletion forces, Eur Biophys J. 37 (2008) 551–561. https://doi.org/10.1007/s00249-007-0255-y.
[59] P. Van Trinh, N.N. Anh, N.T. Tam, N.T. Hong, P.N. Hong, P.N. Minh, B.H. Thang, Influence of defects induced by chemical treatment on the electrical and thermal conductivity of nanofluids containing carboxyl-functionalized multi-walled carbon nanotubes, RSC Adv. 7 (2017) 49937–49946. https://doi.org/10.1039/C7RA08552D.
[60] M. Farbod, A. Ahangarpour, S.G. Etemad, Stability and thermal conductivity of water-based carbon nanotube nanofluids, Particuology. 22 (2015) 59–65. https://doi.org/10.1016/j.partic.2014.07.005.

[61] O.A. Hussein, K. Habib, M. Nasif, R. Saidur, A.S. Muhsan, Investigation of stability, dispersion, and thermal conductivity of functionalized multi-walled carbon nanotube based nanofluid, IOP Conf. Ser.: Mater. Sci. Eng. 863 (2020) 012012. https://doi.org/10.1088/1757-899X/863/1/012012.
[62] Z. Talaei, A.R. Mahjoub, A. morad Rashidi, A. Amrollahi, M. Emami Meibodi, The effect of functionalized group concentration on the stability and thermal conductivity of carbon nanotube fluid as heat transfer media, International Communications in Heat and Mass Transfer. 38 (2011) 513–517. https://doi.org/10.1016/j.icheatmasstransfer.2010.12.035.
[63] H.Q. Xie, H. Lee, W. Youn, M. Choi, Nanofluids containing multiwalled carbon nanotubes and their enhanced thermal conductivities, J. Appl. Phys. 94 (2003) 4967–4971. https://doi.org/10.1063/1.1613374.